4

Fairness Guaranteed Interference Mitigation Scheme in Multi-tier Small Cell Networks

To increase the system capacity, the multi-tier small cell networks have been paid much attention recently. However, the interference issue is a major problem for the densely deployed multi-tier small cell networks. Therefore, a fairness guaranteed interference mitigation scheme has been proposed in this chapter. Both problems and challenges for the interference mitigation scheme have been summarized in detail. Then, the system model and problem formulation are proposed with theoretical analyses in the multi-tier small cell networks scenario. At last, the fairness guaranteed optimal CRE bias and ABS ratio solution has been proposed to mitigate the interference among multi-tier small cells and the performances are verified by numerous results in this chapter.

4.1 Introduction of Problems and Challenges

Recently, the rapid developments on various smart phone applications and different service demands in cellular networks lead to the exponentially surge on mobile traffics. According to statistics, the mobile traffic will grow up to 1,000 times (1,000$\times$) and the user data rate will also increase 10 times (10$\times$) over the next decade in [1]. However, the explosion of mobile traffics brings in both new opportunities and challenges for the cellular network operators. In general, there are three ways to enhance the network capacity: spatial densely deployment, spectral aggregation, and spectrum efficiency improvement. The spatial densely deployment is realized by deploying multi-tier overlaid heterogeneous networks (HetNets) consisting of macrocells and a large number of small cells to improve the network capacity [2]. The spectral aggregation refers to the utilization of carrier aggregation (CA) technology to support a wide system bandwidth up to 100 MHz [3]. In terms of the spectrum efficiency, it can be improved by introducing new transmission technologies such as cooperative multipoint (CoMP) [4] and massive multiple-input multiple-output (MIMO). Among these technologies, the spatial densely deployment scheme is the most effective and low-cost solution, especially in 5G era, to improve the capacity in [5]-[6] by deploying multi-tier heterogeneous cellular networks.

In the multi-tier HetNet scenario, low-power small cells nodes, such as femto, pico, and relay nodes, are overlaid within the coverage of macrocells, which are placed in an unplanned manner in [7]. Compared with macrocell, small cells have a lower transmit power, a smaller coverage, and a lower cost which are easier for operators to maintain and deploy. Small cells can alleviate the traffic pressure of macrocell network by offloading part of the traffics to themselves. However, there are also many problems affecting the capacity enhancement of multi-tier heterogeneous cellular networks. In [8], the cooperative distributed radio resource management algorithms for time synchronization, carrier selection, and power control are discussed for hyper-dense small cells. Traffic imbalance and inter-cell interference among multiple cells are two difficult problems of hyper-dense HetNet which will lead to the inefficient radio resource utilization and affect the capacity and sum data rate in [9].

To solve these problems, both cell range expansion (CRE) and enhanced inter-cell interference coordination (eICIC) technologies are proposed to improve the network capacity of HetNet in the 3GPP Release 8 and Release 9. If the maximum reference signal received power (RSRP) selection principle is applied in the cell association, only a few users can be associated with the low power nodes, which will cause the load imbalance among multiple cells in HetNets and greatly reduce the capacity enhancement by small cells. Adopting the CRE technology in [10], a positive bias value is added to the RSRP of small cell nodes for the cell selection, which can offload part of MUE to small cells and reduce the uplink interference among multi-tier networks. However, these UEs in the cell edge of small cells have a much lower SINR and suffer serious downlink interference from macrocells.

Considering the eICIC technology, it can efficiently improve the range expanded UEs' performance and reduce the inter-cell interference among cells in multi-tier heterogeneous cellular networks. As a time domain interference coordination scheme, the eICIC technology divides time frames into almost blank subframes (ABS) and normal subframes [11]. MUEs and range expanded UEs are scheduled on normal subframes and ABSs orthogonally, which can reduce the interference from macrocells to the range expanded UEs and improve the QoS.

In the literature, the joint usage of CRE and eICIC is proved to be an effective solution to improve the system throughput of HetNet in [12]-[13], but it is much more complicated for the mathematical analysis of network capacity. Besides, if a larger CRE bias of RSRP is applied to reduce the load imbalance among different cells, more ABSs are needed in order to guarantee the performance of range expanded UEs. Therefore, the CRE bias and ABS muting ratio are key parameters that should be configured appropriately to ensure the performance on the interference mitigation and the network capacity enhancement by using the joint CRE and eICIC schemes. In [14], a joint optimization of the CRE bias and radio resources is discussed to ensure the performance of picocells. However, the over-the-air signaling has not been considered yet which leads to the numerical optimization and investigation results unpractical. Moreover, the performance of CRE and eICIC schemes is studied and evaluated by system simulation results in [15], which lacks the mathematical analysis and does not consider about the configuration of CRE and eICIC. Furthermore, the analytical approaches for CRE biasing and eICIC are studied in [16]-[20]. The SINR of HetNet with cell association is studied in [16], but it does not include the resource partitioning scheme and only analyzes the SINR. And the SINR and mean throughput-based analysis for resource partitioning are analyzed in [17]-[18], without considering the user association effect. The optimal CRE bias and ABS ratio scheme are proposed in [19] based on the average spectral efficiency per user. In [20], the joint analysis of resource partitioning and offloading scheme is proposed in terms of the metrics of the effective distribution of SINR, which has no consideration about the optimal parameter configuration effects on UE's fairness. Considering the fairness issue, a graph-based distributed algorithm called fairness guaranteed cooperative resource allocation (FGCRA) is proposed to manage the interference among femtocells in [21], but it only considers the sub-channel allocation which has not considered about the time resources.

Considering the disadvantages of existing works and problems unsolved, a novel eICIC technology is proposed in this chapter by jointly considering the CRE scheme to minimize interferences among multi-tier cellular networks, improve the network throughput, and guarantee the fairness among users. And the poisson point process (PPP) model and two metrics of capacity performance are used including the average capacity per cell and the average capacity per area unit. The optimal CRE bias and ABS ratio are achieved by taking into account the fairness effect of users in multiple cells. Furthermore, the multi-objective decision-making problem is solved by maximizing the proportional fairness (PF) utility [22] and the area capacity of multi-tier heterogeneous cellular networks to realize a tradeoff between fairness and capacity enhancement. Simulations are performed to evaluate the performance of proposed technology. The tradeoff between fairness and network throughput is achieved, when the CRE bias is from 8 to 12 dB and ABS ratio is from 4/8 to 6/8 in [23].

The remainder of this chapter is organized as follows. Both the system model and problem formulation of heterogeneous cellular networks are proposed in Section 4.2. The optimal solution of joint CRE bias and ABS ratio technology is proposed in Section 4.3 by considering about the fairness effect among UEs. Results are discussed and analyzed in Section 4.4. Finally, concluding remarks are described in Section 4.5.

4.2 System Model and Problem Formulation in Multi-tier Small Cell Networks

4.2.1 System Model and Typical Scenario

The typical scenario of multi-tier heterogeneous cellular networks is denoted in Figure 4.1, where picocells are deployed randomly within the coverage of macrocell. To achieve the goal of load balance, CRE technology is proposed to improve the system capacity. However, UEs at the edge of picocell will suffer the strong co-channel interference in downlink from the macrocell. Therefore, in order to minimize the co-channel interference among picocell and macrocell, the eICIC technology is utilized to enhance the performance of picocell user equipment (PUE) by jointly using CRE technology at the cell edge as denoted by PUE_{cre}.

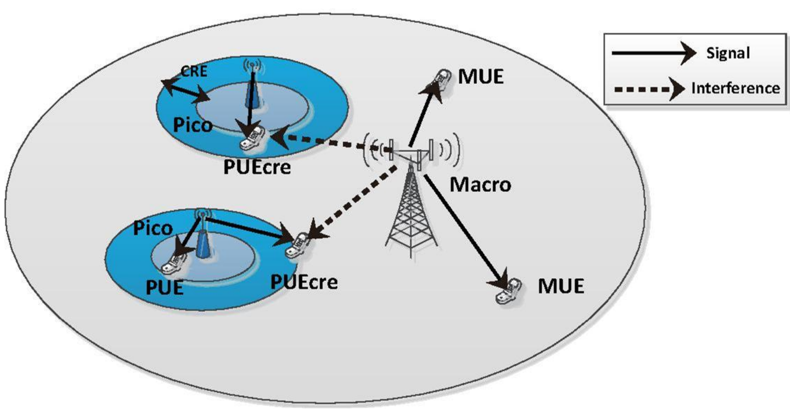

Figure 4.1 *Scenario of multi-tier heterogeneous cellular networks. SOURCE: Reproduced with permission from [23]. Copyright 2015 Springer International Publishing.*

As a time-domain interference coordination mechanism, subframes are divided into ABS and normal subframes. Macrocell mutes its data transmission on specific subframe, where picocell schedules PUE_{cre} on the corresponding subframe to avoid co-channel interferences from macrocell as shown in Figure 4.2.

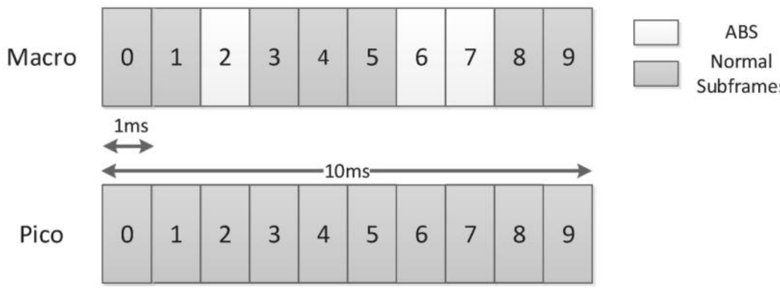

Figure 4.2 *ABS in multi-tier heterogeneous cellular networks scenario. SOURCE: Reproduced with permission from [23]. Copyright 2015 Springer International Publishing.*

4.2.2 Problem Formulation using Cell Association and Resource Partitioning

In the multi-tier heterogeneous cellular networks, the positions of base stations (BSs) are denoted by Φ_k in the kth tier which follows a homogeneous PPP distribution with an intensity of λ_k. And the first tier (k = 1) represents macrocells and the second tier (k = 2) represents picocells. Moreover, the positions of UEs are depicted by Φ_u which follows a homogeneous PPP distribution with an intensity of λ_u and is independent of Φ_k. The transmit power of each BS is assumed as the same and denoted by P_k with a bandwidth of W. And the path loss ratio is $\{\alpha_k\}=4$. Assumed that the multi-tier heterogeneous cellular network is an interference limited system, the inter-cell interference is dominant and the background noise is ignored for analysis simplicity.

In order to offload the high volume traffics from macrocell to small cells, the CRE technology with different CRE bias values is utilized in macrocell and picocell with $B_1 = 0$ dB and $B_2 = B, B > 0$ dB. Considering the cell association relations, different users will choose the appropriate serving BS in the kth tier with the strongest RSRP value as $P_{r,k} = P_k h Z_k^{-\alpha_k} B_k$, where Z_k denotes the distance between UE and BS and h is the channel gain with a Rayleigh distribution, i.e., $h \sim \exp(1)$. Therefore, both the transmit power ratio of BS and the CRE bias ratio of interfering BS to the serving BS are shown in (1).

$$\hat{P}_j = \frac{P_j}{P_k}, \hat{B}_j = \frac{B_j}{B_k} \tag{1}$$

In terms of different CRE bias values, UEs are divided into three types.

Type 1 U_1: MUE associated to k = 1 tier. The RSRP is correspond to $P_{r,1} > BP_{r,2}$.

Type 2 U_2: PUE associated to k = 2 tier at the center of picocell without CRE. The RSRP is correspond to $P_{r,1} < P_{r,2}$.

Type 3 U_{cre}: Picocell UE using CRE (PUE_{cre}) associated to k = 2 tier at the cell edge of picocell with CRE. The RSRP is correspond to $P_{r,2} < P_{r,1} < BP_{r,2}$.

When the ABS configuration ratio is β in the macrocell, the time resource ratio of MUE is denoted by $\rho_1 = 1 - \beta$, and the time resource ratio values of PUEs at the center and cell edge are denoted by $\rho_2 = 1$ and $\rho_{\mathrm{cre}} = \beta$. Moreover, the UEs' proportion of three types is depicted by A_k in (2), and A_1, A_2, and A_{cre} corresponding to U_1, U_2, and U_{cre} are denoted in (3)-(5), which is affected by key parameters including the transmit power, density, and

CRE bias values. Furthermore, the UEs' average number of three types is $N_k = \lambda_u A_k / \lambda_k$ as denoted in (6)-(8).

$$\{A_k\} \overset{\Delta}{=} P\left(\bigcup_{k=1,2\cdots,K_j \neq k} P_{r,k} > P_{r,j} \right) \tag{2}$$

$$A_1 = \frac{\lambda_1 \sqrt{P_1}}{\lambda_1 \sqrt{P_1} + \lambda_2 \sqrt{P_2 B}} \tag{3}$$

$$A_2 = \frac{\lambda_2 \sqrt{P_2}}{\lambda_1 \sqrt{P_1} + \lambda_2 \sqrt{P_2}} \tag{4}$$

$$A_{\text{cre}} = \frac{\lambda_2 \sqrt{P_2 B}}{\lambda_1 \sqrt{P_1} + \lambda_2 \sqrt{P_2 B}} - \frac{\lambda_2 \sqrt{P_2}}{\lambda_1 \sqrt{P_1} + \lambda_2 \sqrt{P_2}} \tag{5}$$

$$N_1 = \frac{\lambda_u \sqrt{P_1}}{\lambda_1 \sqrt{P_1} + \lambda_2 \sqrt{P_2 B}} \tag{6}$$

$$N_2 = \frac{\lambda_u \sqrt{P_2}}{\lambda_1 \sqrt{P_1} + \lambda_2 \sqrt{P_2}} \tag{7}$$

$$N_{\text{cre}} = \frac{\lambda_u \sqrt{P_2 B}}{\lambda_1 \sqrt{P_1} + \lambda_2 \sqrt{P_2 B}} - \frac{\lambda_u \sqrt{P_2}}{\lambda_1 \sqrt{P_1} + \lambda_2 \sqrt{P_2}} \tag{8}$$

To minimize the interference from macrocell to PUEs, the eICIC technology is utilized which is a time resource partitioning approach. The macrocell mutes its transmission on certain fraction of subframes, picocell schedule UEs in the range expanded regions on the corresponding subframes to avoid the interference from the macrocell. Furthermore, macrocell configures its ABS with the ratio β. Thus, the time resource ratio of MUE is $\rho_1 = 1 - \beta$, the time resource ratio of PUE_{cre} is denoted by $\rho_{\text{cre}} = \beta$, and the time resource ratio of PUE that is not affected by ABS is denoted by $\rho_2 = 1$.

Considering the interference that PUE_{cre} suffers from macrocells and other picocells without using the eICIC technology, the SINR of PUE_{cre} is depicted in (9) where BS_{k0} is PUE_{cre}'s serving BS. In contrast, by utilizing the eICIC technology, the SINR of PUE_{cre} only suffer the interference from other picocells, which is depicted in (10). Therefore, the eICIC technology is an effective solution to reduce the interference from macrocell to PUE_{cre} in multi-tier heterogeneous cellular networks.

$$\text{SINR}(x) = \frac{P_2 h_2 x^{-\alpha}}{\sum_{j=1}^{2} \sum_{i \in \phi_j \backslash \text{BS}_{k0}} P_j h_j x^{-\alpha_j}} \tag{9}$$

$$SINR(x) = \frac{P_2 h_2 x^{-\alpha}}{\sum_{i \in \phi_2 \backslash \text{BS}_{k0}} P_2 h_2 x^{-\alpha_2}} \tag{10}$$

Furthermore, X_k denotes the distance between UE and its serving BS in the kth tier in multi-tier heterogeneous cellular networks, and the probability of $X_k > x$ is denoted in (11). And BSs are deployed with a homogeneous PPP distribution model, where X_k is a random variable with the probability density function in (12)-(14) of U_1, U_2, and U_{cre}.

$$P\left(Z_k > x \mid \text{associated to kth tier}\right) = \frac{P\left(Z_k > x\right)}{A_k} \tag{11}$$

$$P(X_k > x) = f_{X_1}(x) = \frac{2\pi\lambda_1}{A_1} x \exp\left[-\pi\left(\lambda_1 + \lambda_2\sqrt{\frac{P_1}{P_2 B}}\right)x^2\right] \tag{12}$$

$$f_{X_2}(x) = \frac{2\pi\lambda_2}{A_2} x \exp\left[-\pi\left(\lambda_2 + \lambda_1\sqrt{\frac{P_1}{P_2}}\right)x^2\right] \tag{13}$$

$$f_{X_{\text{cre}}}(x) = \frac{2\pi\lambda_2}{A_{\text{cre}}} x \left\{ \begin{array}{l} \exp\left[-\pi\left(\lambda_2 + \lambda_1\sqrt{\frac{P_1}{P_2 B}}\right)x^2\right] \\ -\exp\left[-\pi\left(\lambda_2 + \lambda_1\sqrt{\frac{P_1}{P_2}}\right)x^2\right] \end{array} \right\} \tag{14}$$

4.2.3 Interference and Capacity Analysis using CRE and eICIC Technologies

Considering the interference problem of heterogeneous cellular networks, a novel technology by jointly using CRE and eICIC schemes is proposed to improve the system capacity by minimizing the inter-cell interference. Therefore, the downlink capacity per area unit of the joint CRE and eICIC scheme is affected by different key parameters, such as the BS density λ_k, CRE bias *B*, and time resource ρ_k. And the average capacity per area unit is depicted by C_a in (15). ρ_k is the time resource ratio, λ_k is the BS density of the kth tier, R_k is the average ergodic rate in [16], and W_k is the bandwidth of the kth tier.

$$C_a = \sum_{k=1}^{K} \rho_k \lambda_k R_k W_k \tag{15}$$

Moreover, the average ergodic rate of UE of the kth type is depicted by R_k in (16), where *x* is the distance between UE and BS. By applying the CRE scheme, R_k is denoted in (17)-(18) according to [16], where $C_k = \sum_{j=1}^{2} \lambda_j \sqrt{\hat{P}_j \hat{B}_j}, C_{\text{cre1}} = \lambda_2 + \lambda_1 \sqrt{P_1 / P_2 B}$, $C_{\text{cre2}} = \lambda_2 + \lambda_1 \sqrt{P_1 / P_2}$, $C(t) = \sum_{j=1}^{2} \lambda_j \sqrt{\left(e^t - 1\right) \hat{P}_j} \arctan\left(\sqrt{e^t - 1 / \hat{B}_j}\right)$, $C(t)' = \lambda_2 \sqrt{\left(e^t - 1\right)} \arctan\left(\sqrt{e^t - 1}\right)$.

$$R_k \overset{\Delta}{=} E_x \left\{ E_{\text{SINR}_k} \left[\ln\left(1 + \text{SINR}_k(x)\right) \right] \right\} \tag{16}$$

$$R_k = \frac{\lambda_k}{A_k} \int_0^\infty \frac{1}{C_k + C(t)} dt \quad k = 1, 2 \tag{17}$$

$$\begin{aligned} R_k &= \frac{\lambda_k}{A_k} \int_0^\infty \frac{1}{C_k + C(t)} dt R_{\text{cre}} \\ &= \frac{\lambda_2}{A_{\text{cre}}} \int_0^\infty \frac{1}{C_{\text{cre1}} + C(t)} - \frac{1}{C_{\text{cre2}} + C(t)} dt \end{aligned} \tag{18}$$

Furthermore, the eICIC scheme using ABS configuration is utilized in order to decrease inter-cell interference from macrocell BS (MBS) to PUEs. Thus, the average ergodic rate is denoted by R_1', R_2' and R_{cre}' in Equations 19 to 21 of different UE types due to the dynamic changing features of different time resource partitions with eICIC.

$$R_1' = \frac{\lambda_1}{A_1} \int_0^\infty \frac{1}{C_1 + C(t)} dt \tag{19}$$

$$R_2' = (1 - \beta) \frac{\lambda_2}{A_2} \int_0^\infty \frac{1}{C_2 + C(t)} dt + \beta \frac{\lambda_2}{A_2} \int_0^\infty \frac{1}{C_2 + C(t)'} dt \tag{20}$$

$$R_{\mathrm{cre}}{}' = \frac{\lambda_2}{A_{\mathrm{cre}}} \int_0^{\infty} \frac{1}{C_{\mathrm{cre1}} + C(t)'} - \frac{1}{C_{\mathrm{cre2}} + C(t)'} dt \qquad (21)$$

Thus, the proposed CRE bias scheme can realize the load balance among different cells and increase the capacity in multi-tier heterogeneous cellular networks with appropriate CRE bias value configuration. However, PUE_{cre} will suffer the strong interference from MBS in the vicinity. Furthermore, in order to minimize the inter-cell interference, the eICIC technology using ABS ratio configuration is applied to utilize both the temporal and spatial separations among MUEs and PUEs. But, the system capacity of multi-tier heterogeneous cellular networks is affected in terms of the inefficient resource utilization. Thus, how to improve the capacity by considering the tradeoff between CRE bias B and ABS ratio β is a big challenge, which has not been solved yet. In summary, a novel eICIC technology by jointly utilizing CRE bias and ABS ratio scheme is proposed by considering the fairness aspect among different users to minimize the inter-cell interferences among multi-tier heterogeneous cellular networks, improving the network throughput and QoS.

4.3 Fairness Guaranteed Optimal CRE Bias and ABS Ratio Solution

In this section, an optimal CRE bias and ABS ratio scheme is proposed by considering the fairness aspect among different UEs in multi-tier heterogeneous cellular networks. The CRE technology can offload part of MUEs into small cells, and the data rate of a single MUE will improve with the increase of CRE bias value *B*. Thus, the proposed CRE bias scheme can realize the load balance and increase the capacity in multi-tier heterogeneous cellular networks with an appropriate CRE bias value configuration. However, PUE_{cre} will suffer the strong inter-cell interference from MBS. To minimize the interference, the ABS ratio configuration is applied as an eICIC scheme to utilize both temporal and spatial separations among MUEs and PUEs with the capacity deteriorated. To improve the capacity in terms of the tradeoff between CRE bias B and ABS ratio β, an optimal CRE bias and ABS ratio solution is proposed by taking into account the fairness aspect of three types of UEs at different locations within the macrocell. The single UE's average ergodic rate $\bar{R}_k$ of the kth type is denoted in (22), where N_k is the UE's average number per cell in (6)-(8). The joint CRE and eICIC scheme allocates the radio resources to different UEs. Moreover, the tradeoff between system throughput and fairness exists and achieved with numerous results. The proportional fairness utility PF is denoted by (23), and the average capacity per area unit is denoted by C_a in (24).

$$\bar{R}_k = \rho_k \frac{R_k}{N_k} \tag{22}$$

$$\begin{aligned}
\mathrm{PF} &= \sum_{k=1}^{K} A_k \log\left(\bar{R}_k\right) \\
&= \left[\begin{array}{l} A_1 \log\left(\dfrac{(1\text{-}\beta) R_{1_{\mathrm{ICIC}}}}{N_1}\right) \\ + A_2 \log\left(\dfrac{R_{2_{\mathrm{ICIC}}}}{N_2}\right) + A_{\mathrm{cre}} \log\left(\dfrac{\beta R_{\mathrm{cre}_{\mathrm{ICIC}}}}{N_{\mathrm{cre}}}\right) \end{array}\right] \\
&= A_1 \log\left(\frac{\lambda_1^{\,2}(1\text{-}\beta)}{A_1^{\,2}\lambda_u} \int_0^\infty \frac{1}{C_1 + C(t)} dt\right) \\
&+ A_2 \log\left(\frac{\lambda_2^{\,2}(1-\beta)}{A_2^{\,2}\lambda_u} \int_0^\infty \frac{1}{C_2 + C(t)} dt + \frac{\lambda_2^{\,2}\beta}{A_2^{\,2}\lambda_u} \int_0^\infty \frac{1}{C_2 + C(t)'} dt\right) \\
&+ A_{\mathrm{cre}} \log\left(\frac{\lambda_2^{\,2}\beta}{A_{\mathrm{cre}}^{\,2}\lambda_u} \int_0^\infty \frac{1}{C_1 + C(t)'} - \frac{1}{C_2 + C(t)'} dt\right)
\end{aligned} \tag{23}$$

$$
\begin{aligned}
C_a &= \sum_{k=1}^{K} \rho_k A_k R_k W_k = W\left[(1\text{-}\beta) A_1 R_{1_{\text{ICIC}}} + A_2 R_{2_{\text{ICIC}}} + \beta A_{\text{cre}} R_{cre_{ICIC}}\right] \\
&= W\begin{bmatrix} (1\text{-}\beta)\lambda_1 \int_0^{\infty} \frac{1}{C_1 + C(t)} dt + (1-\beta)\lambda_2 \int_0^{\infty} \frac{1}{C_2 + C(t)} dt \\ +\beta\lambda_2 \int_0^{\infty} \frac{1}{C_2 + C(t)'} dt \\ +\beta\lambda_2 \int_0^{\infty} \frac{1}{C_{\text{cre1}} + C(t)'} - \frac{1}{C_{\text{cre2}} + C(t)'} dt \end{bmatrix} \\
&= W\left[(1\text{-}\beta)\int_0^{\infty} \frac{\lambda_1}{C_1 + C(t)} + \frac{\lambda_2}{C_2 + C(t)} dt + \beta\lambda_2 \int_0^{\infty} \frac{1}{C_1 + C(t)'} dt\right] \\
&= W\int_0^{\infty} \frac{(1\text{-}\beta)\lambda_1}{C_1 + C(t)} + \frac{(1\text{-}\beta)\lambda_2}{C_2 + C(t)} + \frac{\beta\lambda_2}{C_1 + C(t)'} dt
\end{aligned}
\tag{24}
$$

The proportional fairness utility was originally proposed in the context of rate control in wired networks [22] by maximizing the logarithmic utility function $y = \sum_{i=1}^{U} \log(T_i)$, where T_i is the throughput of user i and U is the total number of users in the system, which yields a good balance between system throughput and fairness. Therefore, in order to guarantee the fairness of three types of UEs in multi-tier heterogeneous cellular networks, the optimization model is defined as a multi-objective decision making problem in (25) with the constraints of CRE bias B and ABS ratio β, where $F(B,\beta)$ is the objective function, $\phi(B,\beta)$ is the constraint, and CRE bias B and ABS ratio β are variables.

$$
\begin{aligned}
F(B,\beta) &= \begin{cases} \max PF(B,\beta) \\ \max C_a(B,\beta) \end{cases} \\
\text{s.t.}\,\phi(B,\beta) &= \begin{cases} 0dB \le B \le 2\text{dB} \\ 1/8 \le \beta \le 7/8 \end{cases}
\end{aligned}
\tag{25}
$$

Generally, the multi-objective functions cannot reach the same maximum at the same time. Therefore, to solve the multi-objective optimization problem, the lexicographic method is applied which sorts the objective functions according to their importance. The optimal solution of the *m*th objective is based on the previous optimal solution of (*m*-1)th objective. Thus, the multi-objective optimal solution for (25) is achieved finally in (26). Because, the fairness guarantee is more important than capacity improvement, we choose to maximize the PF as the first objective and the C_a as the second objective. In addition, the lexicographic method can reduce almost half the amount of calculations, guarantee the fairness, and improve the capacity. The optimal fairness based CRE bias and ABS ratio solution is shown in Algorithm 1.

$$
\begin{aligned}
& f_1(\{B,\beta\}^{(1)}) = \max_{\{B,\beta\}\in R_0} \mathrm{PF}(B,\beta) \\
& f_2(\{B,\beta\}^{(2)}) = \max_{\{B,\beta\}\in R_1} C_a(B,\beta) \\
& R_1 = \left\{\{B,\beta\} \mid \{B,\beta\}\in R_0\right\} \\
& R_0 = \{B,\beta\} = \{[0dB, 20dB],[1/8, 7/8]\}
\end{aligned}
\tag{26}
$$

Algorithm 1 Optimal CRE bias and ABS ratio solution based on fairness

Input:
The macrocell and picocell density λ_1, λ_2.
The macro BS and pico BS transmit power P_1, P_2.
The UE density λ_u.
Output:
1: **for** each $B \in [0, 20]dB$ **do**
2: **for** each $\beta \in [1/8, 7/8]$ **do**
3: Calculate the proportional fairness utility PF by (23).
4: Find the max PF and output the first step objective optimal solution $R_0 = [B, \beta]$.
5: **end for**
6: **end for**
7: **for** each $B \in R_0$ **do**
8: **for** each $\beta \in R_0$ **do**
9: Calculate the average capacity per area unit C_a by (24).
10: Find the max C_a and output the second step objective optimal solution $R_1 = [B, \beta]$.
11: **end for**
12: **end for**
13: **return** The optimal CRE bias B and ABS ratio β.

4.4 Results and Performance Analyses

In this section, numerical simulations are performed with different scenarios and results are analyzed thoroughly. Macrocells and picocells are deployed with densities of $\lambda_1 = 4.62$ and $\lambda_2 = K_P \lambda_1$ BS/km^2, respectively. And the transmit power for macrocell and picocell is $P_1 = 46$ dBm and $P_2 = 30$ dBm. The system bandwidth is defined by $W = 10$ MHz, and the path loss exponent is denoted by $\alpha = 4$.

4.4.1 Capacity Analysis of Stand-alone Effects by BS Density, CRE, and eICIC

Considering different parameters that affect the performance of system capacity in multi-tier heterogeneous cellular networks, key parameters, such as the BS density, CRE, and eICIC, are discussed with numerical results in terms of different ratios of PUE and system throughput of various cells.

In terms of the effects of BS density and CRE bias values to the system capacity, results are discussed and analyzed thoroughly below. First, the traffic offloading from macrocells to picocells is depicted in Figure 4.3. The PUE's ratio increases with the surge of CRE bias value when the picocell's density is constant. With the increase of picocell's density, PUE's ratio will also increase. By using the CRE technology, the over-loaded macrocell can offload part of its traffic to picocells which can realize a load balance in multi-tier heterogeneous cellular networks.

Besides, Figure 4.4 depicts the effect of CRE bias and picocell's density on the average capacity per cell under different CRE bias values. As the CRE bias increases, more MUEs with a low SINR value are associated with picocells and the PUE_{cre} are associated to BSs that are not offering the strongest received signal to minimize the inter-cell interference. Therefore, with the increase of CRE bias, the throughput of macrocells increases and the average throughput of picocells decreases.

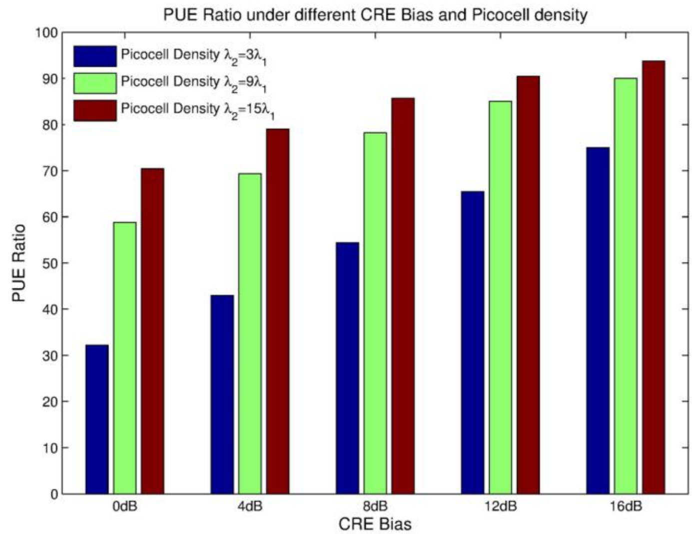

Figure 4.3 *PUE's ratio under different CRE bias and picocell's density. SOURCE: Reproduced with permission from [23]. Copyright 2015 Springer International Publishing.*

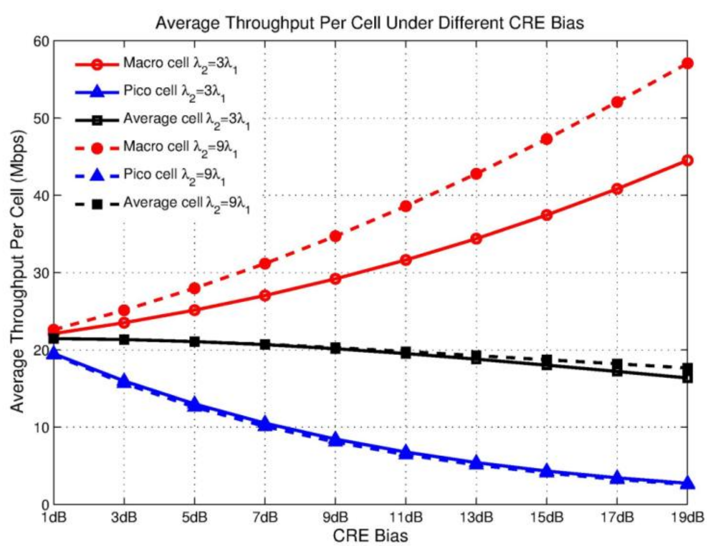

Figure 4.4 *The average capacity per cell under different CRE bias. SOURCE: Reproduced with permission from [23]. Copyright 2015 Springer International Publishing.*

In terms of the effect of utilizing the eICIC technology to the system capacity, Figure 4.5 denotes the relation of ABS ratio and picocell's density on the average throughput per cell. As the ABS ratio increases, more MUEs are mute on specific subframes, which provide more PUE_{cre} with more time resources. Therefore, with the increase of ABS ratio, the throughput of macrocell decreases and the throughput of picocell increases due to the efficient time-domain resource configuration among macrocell and picocell.

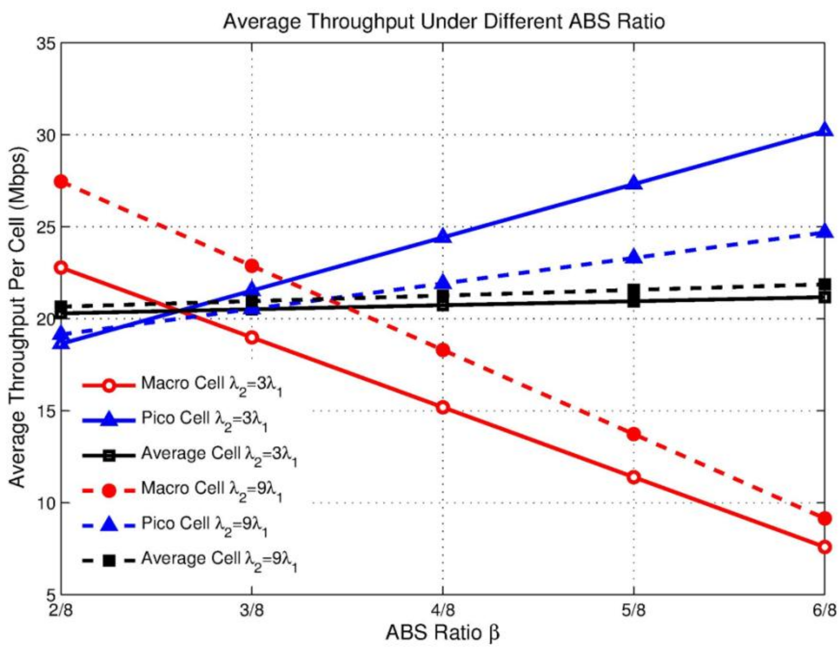

Figure 4.5 *The average capacity per cell under different ABS ratio. SOURCE: Reproduced with permission from [23]. Copyright 2015 Springer International Publishing.*

4.4.2 Optimal CRE Bias and ABS Ratio Technology

The average capacity per area is depicted in Figure 4.6 in multi-tier heterogeneous networks, which increases as the picocell's density increases. The joint CRE and eICIC scheme can improve the network capacity. In order to provide the service with a requirement of 1.3 Gbps/km^2 in the 10 MHz bandwidth system, the picocell's density is about 55 BS/km^2 without using CRE and eICIC, which is about 12 times higher than macrocell's density. Importantly, by using the CRE and eICIC scheme, the picocell's density decreases significantly to 30 BS/km^2 (about 6 times higher than macrocell's density) which can minimize the inter-cell interference among macrocells and densely deployed picocells. In addition, under the same picocell's density, the joint CRE and eICIC technology can improve the network capacity over 40%.

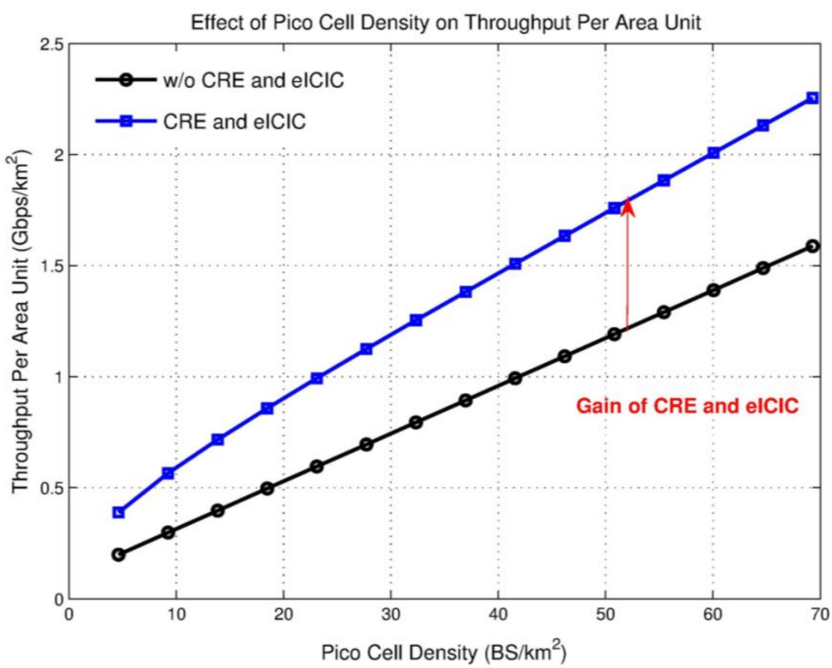

Figure 4.6 *Effect of picocell's density to average capacity per area unit with/without CRE and eICIC. SOURCE: Reproduced with permission from [23]. Copyright 2015 Springer International Publishing.*

Furthermore, the fairness effect is considered by PF utility value, which is a function of CRE bias and ABS ratio values in Figure 4.7. The PF utility can achieve the optimal value with the increase of CRE bias and ABS ratio values.

Moreover, the average capacity increases with the increase of ABS ratio values in Figure 4.8. And the average capacity decreases as CRE bias becomes larger.

By utilizing the lexicographic method, the optimal CRE bias and ABS ratio are achieved in the multi-tier heterogeneous cellular networks. In the case of picocell's density $\lambda_2 = 6\lambda_2$, the PF utility has little difference when the CRE bias is from 8 to 12 dB and ABS ratio is from 3/8 to 6/8 in Figure 4.7. In order to maximize the average capacity per cell, the optimal CRE bias is 12 dB and ABS ratio is 6/8. Similarly, when the picocell's density $\lambda_2 = 12\lambda_2$, the optimal CRE bias is 10 dB and ABS ratio is 5/8. In addition, the optimal CRE bias and ABS ratio are less affected by picocell's density. Therefore, simulation results show that when the CRE bias is from 8 to 12 dB and ABS ratio is from 4/8 to 6/8 the optimal solution is achieved and it can improve the capacity by 40% in terms of the fairness among different UEs.

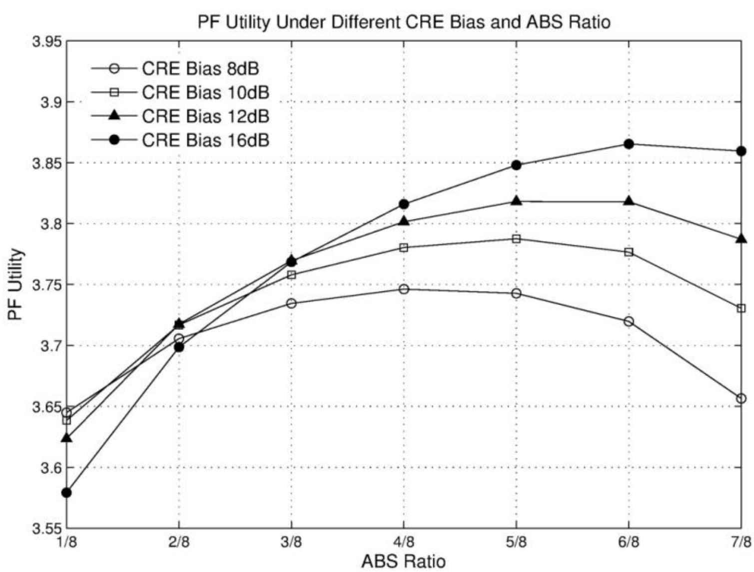

Figure 4.7 *PF utility with different CRE bias and ABS ratio. SOURCE: Reproduced with permission from [23]. Copyright 2015 Springer International Publishing.*

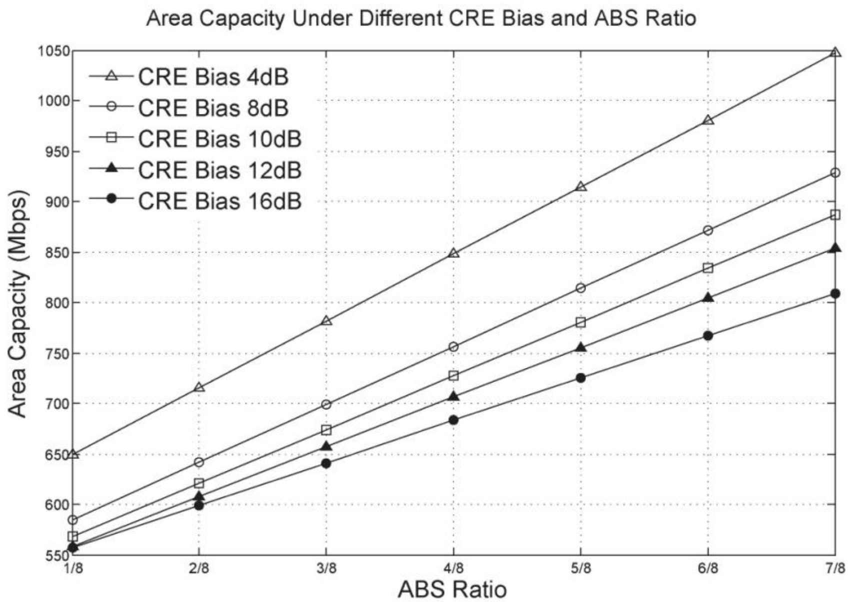

Figure 4.8 *Average capacity with different CRE bias and ABS ratio. SOURCE: Reproduced with permission from [23]. Copyright 2015 Springer International Publishing.*

4.4.3 System-Level Simulation Results of Novel eICIC Technology

A typical network layout designed as defined in [7] with the co-channel deployment of macrocells and picocells. The network topology consists of the standard three-sector macro BSs, complemented with a set of four pico BSs per sector in Figure 4.9. For the scenarios by using the CRE and eICIC enabled technologies, we assume that CRE bias 10 dB and ABS ratio 5/8 are suitable for all picocell BSs. UEs are assumed to be LTE Release 10 compliant, so they can support the separate CSI values report for ABS and non-ABS subframes. The default simulation parameters are summarized in Table 4.1.

***Table 4.1** Simulation parameters. SOURCE: Reproduced with permission from [23]. Copyright 2015 Springer International Publishing.*

	Macrocell	**Picocell**
Cellular layout	19 cell sites, 3 sectors per site	4 picocells per sector
Number of UEs	60 per macro cell	60 per macro cell
Distance-dependent path loss	ITU urban macro(UMa)[7]	ITU urban micro(UMi) [7]
Shadowing standard deviation	8 dB	10 dB
Penetration loss	0 dB	0 dB
Total eNodeB Tx power	46 dBm	30 dBm
Antenna configuration	2 × 2 (uncorrelated)	2 × 2 (uncorrelated)
Antenna pattern	3D	2D
Antenna height	25 m	10 m
Antenna gain	14 dBi	5 dBi
Carrier frequency	2 GHz	2 GHz
System bandwidth	10 MHz	10 MHz
Traffic model	Full buffer, full load	Full buffer, full load

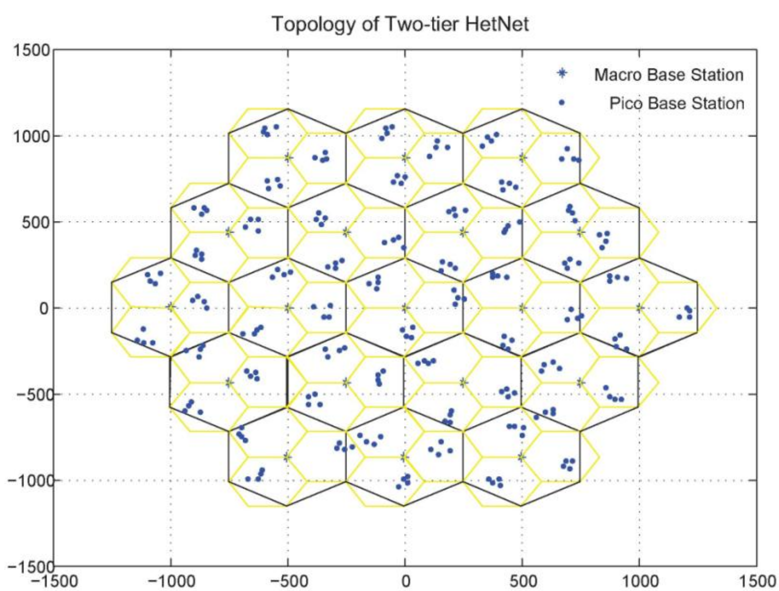

***Figure 4.9** The network topology of two-tier HetNet. SOURCE: Reproduced with permission from [23]. Copyright 2015 Springer International Publishing.*

Figure 4.10 shows the cumulative distribution function (CDF) of PUE's SINR. By using the eICIC technology, the SINR of PUEs can be improved because PUEs are scheduled on ABSs without the interference from macrocells with the appropriate ABS configuration.

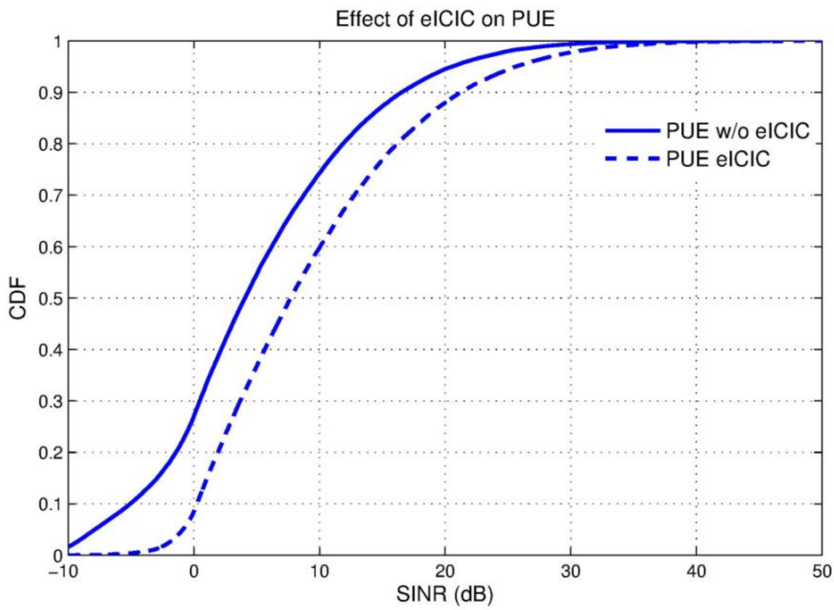

Figure 4.10 *Cumulative distribution function of PUE's SINR. SOURCE: Reproduced with permission from [23]. Copyright 2015 Springer International Publishing.*

Figure 4.11 shows the CDF of throughput of different UEs. By using the CRE and eICIC technology, both the throughput of PUE and the average throughput increase. However, the throughput of MUE will decrease because of limited time resources. Furthermore, the throughput gap between MUE and PUE is decreased, which depicts a better fairness than the scenario without using CRE and eICIC technologies. In a word, the joint CRE and eICIC scheme can improve the throughput and the fairness among different UEs.

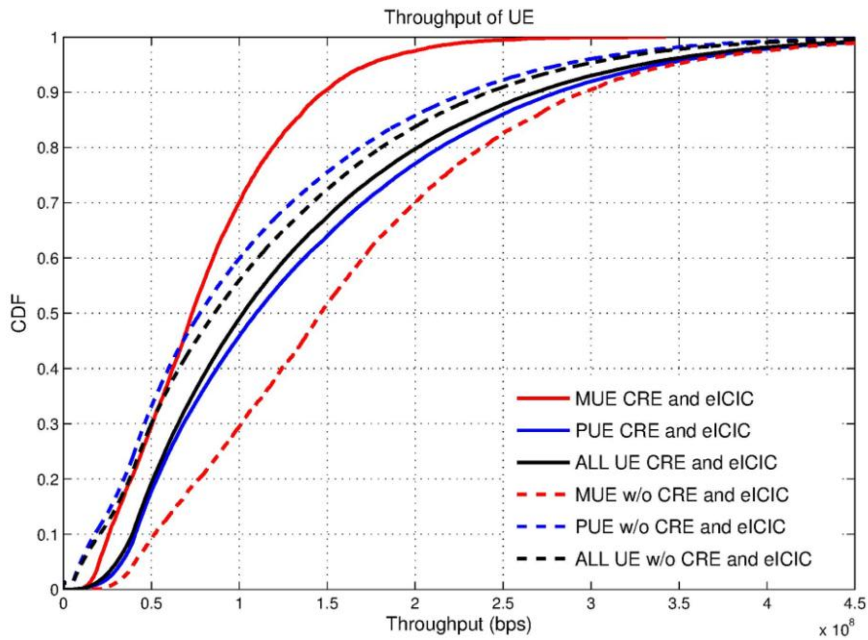

Figure 4.11 *Cumulative distribution function of throughput for different UEs. SOURCE: Reproduced with permission from [23]. Copyright 2015 Springer International Publishing.*

4.5 Concluding Remarks

In this chapter, the joint CRE and eICIC scheme is proposed to minimize the inter-cell interference in the multi-tier heterogeneous cellular networks. And the optimal CRE bias and ABS ratio solutions are achieved by taking into account the fairness effect among different UEs. The multi-objective decision-making scheme is designed to maximize the PF utility and the area capacity. Simulation results show that when the CRE bias is from 8 to 12 dB and ABS ratio is from 4/8 to 6/8, the optimal solution is achieved which can improve the capacity by 40%, which considers about the fairness among different UEs.

References

[1] P. Mogensen et al, “B4G local area: high level requirements and system design”, *in Proc. IEEE Globecom Workshops*, Anaheim, CA, pp. 613-617, Dec. 2012.

[2] N. Bhushan et al, “Network densification: the dominant theme for wireless evolution into 5G”, *IEEE Commun. Mag.*, vol. 52, no. 2, pp. 82-89, Feb. 2014.

[3] M. A. M. Al-Shibly, M. H. Habaebi and J. Chebil, “Carrier aggregation in Long Term Evolution-Advanced”, *in Proc. IEEE ICSGRC*, Shah Alam, Selangor, pp. 154-159, Jul. 2012.

[4] A. Davydov, G. Morozov, I. Bolotin and A. Papathanassiou, “Evaluation of joint transmission CoMP in C-RAN based LTE-A HetNets with large coordination areas”, *in Proc. IEEE Globecom Workshops*, Atlanta, GA, pp. 801-806, Dec. 2013.

[5] S. Parkvall, E. Dahlman, G. Jöngren, S. Landström, L. Lindbom, “Heterogeneous network deployments in LTE”, Ericsson Review, Jan. 2011.

[6] K. Hiltunen, “Comparison of different network densification alternatives from the LTE downlink performance point of view”, *in Proc. IEEE VTC Fall*, San Francisco, CA, pp. 1-5, Sept. 2011.

[7] “Evolved universal terrestrial radio access (E-UTRA); further advancements for E-UTRA physical layer aspects (Release 9)”, 3GPP TR 36.814, 3rd Generation Partnership Project (3GPP), 2010.

[8] J. Xu, J. Wang, Y. Zhu, et al., “Cooperative distributed optimization for the hyper-dense small cell deployment”, *IEEE Commun. Mag.*, vol. 52, no. 5, pp. 61-67, May 2014.

[9] Hwang, B. Song and S. S. Soliman, “A holistic view on hyper-dense heterogeneous and small cell networks”, *IEEE Commun. Mag.*, vol. 51, no. 6, pp. 20-27, Jun. 2013.

[10] “Range expansion for efficient support of heterogeneous networks”, 3GPP R1-083813, 2008.

[11] “Comparison of time-domain eICIC solutions”, 3GPP R1-104661, 2010.

[12] Okino, T. Nakayama, C. Yamazaki, H. Sato and Y. Kusano, “Pico cell range expansion with interference mitigation toward LTE-Advanced heterogeneous networks”, *in Proc. IEEE ICC Workshops*, Kyoto, pp. 1-5, Jun. 2011.

[13] M. Vajapeyam, A. Damnjanovic, J. Montojo, T. Ji, Y. Wei and D. Malladi, “Downlink FTP performance of heterogeneous networks for LTE-Advanced”, *in Proc. IEEE ICC Workshops*, Kyoto, pp. 1-5, Jun. 2011.

[14] R. Madan, J. Borran, A. Sampath, N. Bhushan, A. Khandekar and T. Ji, “Cell association and interference coordination in heterogeneous LTE-A cellular networks”, *IEEE J. Sel. Areas Commun.*, vol. 28, no. 9, pp. 1479-1489, Dec. 2010.

[15] M. Shirakabe, A. Morimoto and N. Miki, “Performance evaluation of inter-cell interference coordination and cell range expansion in heterogeneous networks for LTE-Advanced downlink”, *in Proc. ISWCS, Aachen*, pp. 844-848, Nov. 2011.

[16] H. S. Jo, Y. J. Sang, P. Xia and J. G. Andrews, “Heterogeneous cellular networks with flexible cell association: a comprehensive downlink SINR analysis”, *IEEE Trans. Wireless Commun.*, vol. 11, no. 10, pp. 3484-3495, Oct. 2012.

[17] T. D. Novlan, R. K. Ganti, A. Ghosh and J. G. Andrews, “Analytical evaluation of fractional frequency reuse for heterogeneous cellular networks”, *IEEE Trans. Commun.*, vol. 60, no. 7, pp. 2029-2039, Jul. 2012.

[18] M. Cierny, H. Wang, R. Wichman, Z. Ding and C. Wijting, “On number of almost blank subframes in heterogeneous cellular networks”, *IEEE Trans. Commun.*, vol. 12, no. 10, pp. 5061-5073, Oct. 2013.

[19] S. Mukherjee and İ Güvenç, “Effects of range expansion and interference coordination on capacity and fairness in heterogeneous networks”, *in Proc. ASILOMAR*, Pacific Grove, CA, pp. 1855-1859, Nov. 2011.

[20] S. Singh and J. G. Andrews, “Joint resource partitioning and offloading in heterogeneous cellular networks”, *IEEE Trans. Wireless Commun.*, vol. 13, no. 2, pp. 888-901, Feb. 2014.

[21] S. Wang, J. Wang, J. Xu, Y. Teng, K. Horneman, “Fairness guaranteed cooperative resource allocation in femtocell networks”, *Wireless Pers. Commun.*, vol. 72, no. 2, pp. 957–973, Sept. 2013.

[22] F. Kelly, “Charging and rate control for elastic traffic”, *Euro Trans. Telecommun.*, vol. 8, no. 1, pp. 33-37, Jan. 1997.

[23] Q. Zhang, T. Yang, Y. Zhang, “Fairness guaranteed novel eICIC technology for capacity enhancement in multi-tier heterogeneous cellular networks”, *EURASIP J. Wireless Comm. and Networking*, 2015 (62), pp. 1-12, Feb. 2015.